Universiteit Utrecht

Faculteit Bètawetenschappen

The shape of a magnonic black hole horizon

Bachelor Thesis

Bram van de Zande

Natuur- en Sterrenkunde

Supervisor:

Dr. R. Duine
Theoretical physics

12-06-2019

Abstract

Black holes are extremely dense objects with a gravitational field so strong that nothing, not even light, can escape from it. One of Stephen Hawkings most popular findings is that black holes might, in fact, be not completely black and emit radiation caused by quantum effects at the horizon which is called Hawking radiation. Black holes are for obvious reasons really hard to detect and creating one is out of our reach, so analogue systems are proposed to test the theory of Hawking radiation. One of those analogues is a magnonic black hole system. Magnons are spin-waves in a ferromagnetic material. If a current is induced, the magnons act like particles in a gravitational field. We design a model for different shaped electrical circuits made of magnetic material where we make use of the Laplace equation and corresponding boundary conditions to simulate such a black hole and determine the shape of its horizons. We find that the shape of the magnonic black hole horizon depends on the geometry of the ferromagnetic system and the magnitude of the applied current. The results may be helpful for the experimental design of magnonic black holes.

Contents

1 Introduction

Black holes are amongst the most extreme and fascinating objects in the universe. In 1783, John Mitchel proposed the idea of an object with a strong enough gravitational pull so that matter or even light would not be able to escape it [1]. Until recently, black holes existed just as a theoretical idea, without any proof or observation of their real existence. This changed when LIGO detected gravitational waves whose frequency matched perfectly with a binary black hole merger[2]. Even more recently, the Event Horizon Telescope succeeded in making an image of the super massive black hole at the centre of galaxy M87[3]. Although we have managed to proof the existence of black holes, raw data of black holes remains scarce, as they are so hard to detect. Therefore, almost all knowledge on black holes results from theories, whose consistency with real life has yet to be tested. The most interesting property of a black hole is its point of no return, the boundary where nothing, not even light, can escape the black hole, called the horizon. At this boundary a phenomena called Hawking radiation might occur. Stephen Hawking proposed that at the black hole horizon a particle and anti-particle can be created due to quantum effects. When the particles are just in- and outside the event horizon, the particles won't be able to annihilate again and one of the two particles escapes the black hole. Hawking showed that this radiation is black-body radiation and thus corresponds to the temperature of the black hole. This temperature is also known as the Hawking temperature. By this process, the black hole loses energy, and thus mass. When no mass is falling in the black hole, the black hole will vaporize by this process and eventually die. Unfortunately, experimental testing on a black hole's horizon is out of our reach, but in 1981 Unruh proposed a system where a black hole can be simulated. He proposed that in a flowing fluid, different regions can be created where sound waves can or cannot exceed the velocity of the fluid itself, creating a subsonic and supersonic region, respectively. Such a system is called a sonic black hole. The boundary between the sub and supersonic region is the horizon[4]. Publishing this paper has led to proposals of various other systems where such horizons are present. These system are called black-hole-analogues and can be found in different fields of physics. For example, Oren Lahav *et al.* succeeded in creating a sonic black hole in an Bose-Einstein condensate [5] and Rousseaux *et al.* created a black hole analogue in a water tank [6]. They directly observed the conversion of incident waves with positive- into negative-frequency waves in a moving medium. A conversion like that also occurs at the event horizon of a black hole. In 2017, Duine *et al.* proposed a black-hole-analogue in the field of condensed matter[7]. They found that in an electrical circuit made of ferromagnetic material, a 'subsonic' and 'supersonic' region can be created by narrowing the geometry of the circuit. It is at this boundary where the magnonic horizon is located. As they stated in their paper, magnonic black holes are attractive, since the system can be embedded in a device, can be electrically contacted, and has properties that are controlled by magnetic fields and electrical currents.

So far, the study of magnonic black holes is at its infancy. More research needs to be done to elucidate the general properties of a magnonic black hole, before meaningful experiments can be initiated. So far, properties like the dispersion relation [8] and Cherenkov radiation [9] have been studied. While it is clear that the system does have a horizon, its actual shape remains unclear. To experimentally test properties like Hawking and Cherenkov radiation, it is important to know the exact location and shape of the horizon, since the radiation is

produced at the horizon. The wavelengths of the Hawking radiation must be known to a high level of precision to determine its corresponding Hawking temperature.

In this thesis, we first provide insight in spin-waves and derive its velocity from the Landau-Lifschitz-Gilbert equation, to show the analogy between spin-waves and gravity and hence with black-holes. In the second section we define two magnonic black hole models and show the results of the current density of the models. From this, we can determine the shape of the magnonic black hole horizon. We find that the shape of the horizons are mainly smoothly curved, where the location and degree of curvature depends on the length scale and the value of the critical density. Finally, we discuss the results and suggest further research.

2 Magnons

Each atom consists of protons, neutrons and electrons, where exact quantities of these determine the properties of the atom. Each electron has an intrinsic angular momentum which is called spin, and can have two possible values. It can be either $+\hbar/2$ (spin up) or $-\hbar/2$ (spin down). If an atom has multiple electrons, these spins can add up, resulting in a total spin of the atom and thus a magnetic moment. In a ferromagnetic material, it is energetic favourable for atoms to align their spin with their neighboring atoms. If thermal energy is reduced so that the system is below its Curie temperature, the system will occupy the ground state. In the ground state of a ferromagnetic material, all the spins align and this will result in a total magnetic field. If some energy is added to the system, states other than the ground state are occupied. Not all spins are perfectly aligned anymore and spins are now under a small angle with the magnetic field, resulting in a torque on the spins, causing precession. Also neighboring spins exert a torque on each other, which leads to a dynamic system where the precession of neighboring spins are out of phase. Yet the rate of precession is in sync which leads to spin-waves in the material. These spin-waves are also called magnons and can be seen in Figure 1.

How spins behave in the presence of an external magnetic field and a spin polarized electrical current is described by the Landau-Lifschitz-Gilbert equation (LLG equation). In the next section we give a detailed calculation of the velocity of magnons in a ferromagnet using the LLG equation and show the analogy with gravity.

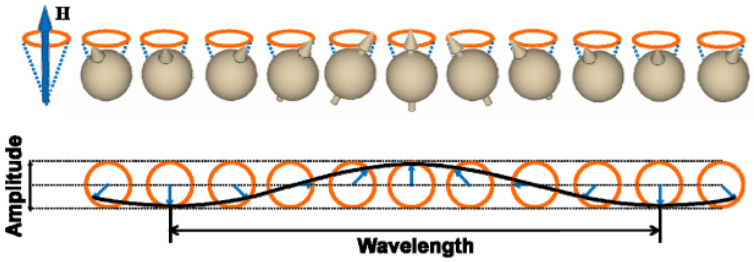

Figure 1: Visualization of a spin-wave in one dimension. Taken from [10].

2.1 The Landau-Lifschitz-Gilbert equation

The Landau-Lifschitz-Gilbert equation is an equation for the magnetization direction in a ferromagnet. Without dissipative terms, it is given by [7]

$$i\hbar(\partial_t + \boldsymbol{v_s}\cdot\boldsymbol{\nabla})\psi = (-J_s\nabla^2 - \mu + g|\psi|^2)\psi, \tag{2.1}$$

where $\hbar$ is the reduced Planck's constant, J_s the spin stiffness, μ the effective chemical potential given by $\mu = K - B$, where K is the anisotropy constant and B the external magnetic field. Furthermore, g is the Landé factor and ψ the complex field related to the magnetization direction $\boldsymbol{m}$ as

$$\boldsymbol{m} = (\sqrt{\mu_B/2M_s}Re[\psi], \sqrt{\mu_B/2M_s}Im[\psi], 1 - \mu_B|\psi|^2/M_s), \tag{2.2}$$

and $\boldsymbol{v_s}$ the spin-drift velocity. This is the average spin-velocity a stream of charged particles attain in an electric field and is given by

$$\boldsymbol{v_s} = -\frac{gP\mu_B\boldsymbol{j}}{2eM_s}, \tag{2.3}$$

where P the spin polarization of the current, μ_B the Bohr magneton, $\boldsymbol{j}$ the electrical transport-current density, e minus the electric charge and M_s the saturation magnetization.

We will now use the ansatz

$$\psi = \sqrt{\rho_0 + \delta\rho(\mathbf{x}, t)}e^{i\Theta(\mathbf{x},t)}, \tag{2.4}$$

where $\delta\rho$ is a small variation on the constant ρ_0. To maintain clarity we will work out all terms of Eq. 2.1 individually, beginning with the first term on the left-hand side and get

$$\begin{aligned} i\hbar\partial_t\psi &= \frac{i\hbar}{2\sqrt{\rho_0+\delta\rho}}e^{i\Theta}\partial_t\delta\rho - \hbar\sqrt{\rho_0+\delta\rho}e^{i\Theta}\partial_t\Theta \\ &= \psi\left[\frac{i\hbar\partial_t\delta\rho}{2(\rho_0+\delta\rho)} - \hbar\partial_t\Theta\right] \\ &= \psi\left[\frac{i\hbar\partial_t\delta\rho}{2\rho_0} - \hbar\partial_t\Theta\right], \end{aligned} \tag{2.5}$$

where we have used that $\delta\rho \ll \rho_0$. The second term on the left-hand side becomes

$$\begin{aligned} i\hbar(\boldsymbol{v_s}\cdot\boldsymbol{\nabla})\psi &= i\hbar(v_x\partial_x + v_y\partial_y + v_z\partial_z)\sqrt{\rho_0+\delta\rho}e^{i\Theta} \\ &= \frac{i\hbar v_x(\partial_x\delta\rho)e^{i\Theta}}{2\sqrt{\rho_0+\delta\rho}e^{i\Theta}} - \hbar v_x\sqrt{\rho_0+\delta\rho}e^{i\Theta}\partial_x\Theta \\ &+ \frac{i\hbar v_y(\partial_y\delta\rho)e^{i\Theta}}{2\sqrt{\rho_0+\delta\rho}e^{i\Theta}} - \hbar v_y\sqrt{\rho_0+\delta\rho}e^{i\Theta}\partial_y\Theta \\ &+ \frac{i\hbar v_z(\partial_z\delta\rho)e^{i\Theta}}{2\sqrt{\rho_0+\delta\rho}e^{i\Theta}} - \hbar v_z\sqrt{\rho_0+\delta\rho}e^{i\Theta}\partial_z\Theta \\ &= \psi\left[\frac{i\hbar}{2\rho_0}(v_x\partial_x + v_y\partial_y + v_y\partial_y)\delta\rho - \hbar(v_x\partial_x + v_y\partial_y + v_y\partial_y)\Theta\right] \\ &= \psi\left[\frac{i\hbar(\boldsymbol{v_s}\cdot\boldsymbol{\nabla})}{2\rho_0}\delta\rho - \hbar(\boldsymbol{v_s}\cdot\boldsymbol{\nabla})\Theta\right]. \end{aligned} \tag{2.6}$$

The first term on the right-hand side becomes

$$J_s \nabla^2 \psi = (\partial_x^2 + \partial_y^2 + \partial_z^2)\sqrt{\rho_0 + \delta\rho} e^{i\Theta}. \tag{2.7}$$

The second order derivative of ψ with respect to x is given by

$$\begin{aligned}
\partial_x^2 \sqrt{\rho_0 + \delta\rho} e^{i\Theta} &= \partial_x \left(\frac{(\partial_x \delta\rho) e^{i\Theta}}{2\sqrt{\rho_0 + \delta\rho}} + \sqrt{\rho_0 + \delta\rho} i e^{i\Theta} \partial_x \Theta \right) \\
&= -\frac{(\partial_x \delta\rho)^2 e^{i\Theta}}{4(\rho_0 + \delta\rho)^{3/2}} + \frac{(\partial_x^2 \delta\rho) e^{i\Theta}}{2\sqrt{\rho_0 + \delta\rho}} + \frac{(\partial_x \delta\rho) i e^{i\Theta} \partial_x \Theta}{2\sqrt{\rho_0 + \delta\rho}} \\
&+ \frac{(\partial_x \delta\rho) i e^{i\Theta} \partial_x \Theta}{2\sqrt{\rho_0 + \delta\rho}} + \sqrt{\rho_0 + \delta\rho} (\partial_x^2 \Theta) i e^{i\Theta} - \sqrt{\rho_0 + \delta\rho} e^{i\Theta} (\partial_x \Theta)^2.
\end{aligned} \tag{2.8}$$

Since the derivatives of $\delta\rho$ and Θ are small, we now neglect second order terms of them. This leads to

$$\begin{aligned}
\partial_x^2 \sqrt{\rho_0 + \delta\rho} e^{i\Theta} &= \frac{(\partial_x^2 \delta) \rho e^{i\Theta}}{2\sqrt{\rho_0 + \delta\rho}} + \sqrt{\rho_0 + \delta\rho} (\partial_x^2 \Theta) i e^{i\Theta} \\
&= \psi \left[\frac{\partial_x^2 \delta\rho}{2\rho_0} + i \partial_x^2 \Theta \right].
\end{aligned} \tag{2.9}$$

Since the derivatives of ψ with respect to y and z are analogue, we combine these to get

$$\begin{aligned}
(\partial_x^2 + \partial_y^2 + \partial_z^2)\sqrt{\rho_0 + \delta\rho} e^{i\Theta} &= \psi \left[\frac{(\partial_x^2 + \partial_y^2 + \partial_z^2)\delta\rho}{2\rho_0} + i(\partial_x^2 + \partial_y^2 + \partial_z^2)\Theta \right] \\
&= \psi \left[\frac{\nabla^2 \delta\rho}{2\rho_0} + i \nabla^2 \Theta \right].
\end{aligned} \tag{2.10}$$

By minimizing the energy we can show that $-\mu + g\rho_0 = 0$. Taking this into account, we write the last two terms as

$$\begin{aligned}
-\mu + g \mid \psi \mid^2 &= -\mu + g(\rho_0 + \delta\rho) \\
&= g\delta\rho.
\end{aligned} \tag{2.11}$$

Putting this all together and dividing all terms by ψ, we write Eq. 2.1 as

$$i\hbar \frac{\partial_t + (\boldsymbol{v_s} \cdot \boldsymbol{\nabla})}{2\rho_0} \delta\rho - \hbar(\partial_t + (\boldsymbol{v_s} \cdot \boldsymbol{\nabla}))\Theta = -J_s \left[\frac{\nabla^2 \delta\rho}{2\rho_0} + i\nabla^2 \Theta \right] + g\delta\rho. \tag{2.12}$$

Taking the real and imaginary part of this equation gives us two equations. The real part is given by

$$-\hbar(\partial_t + (\boldsymbol{v_s} \cdot \boldsymbol{\nabla}))\Theta = -J_s \frac{\nabla^2 \delta\rho}{2\rho_0} + g\delta\rho, \tag{2.13}$$

and the imaginary part by

$$\hbar \frac{\partial_t + (\boldsymbol{v_s} \cdot \boldsymbol{\nabla})}{2\rho_0} \delta\rho = -J_s \nabla^2 \Theta. \tag{2.14}$$

We now apply the operator $\partial_t + (\boldsymbol{v_s} \cdot \boldsymbol{\nabla})$ to Eq. 2.14. This gives

$$\hbar[\partial_t + (\boldsymbol{v_s} \cdot \boldsymbol{\nabla})]\frac{\partial_t + (\boldsymbol{v_s} \cdot \boldsymbol{\nabla})}{2\rho_0}\delta\rho = -J_s[\partial_t + (\boldsymbol{v_s} \cdot \boldsymbol{\nabla})]\nabla^2\Theta. \tag{2.15}$$

Since Θ is a smooth function, we change the order of derivatives. By moving the ∇^2 operator on the right-hand side to the front, we plug Eq. 2.13 into the above to obtain

$$\hbar^2[\partial_t + (\boldsymbol{v_s} \cdot \boldsymbol{\nabla})]\frac{\partial_t + (\boldsymbol{v_s} \cdot \boldsymbol{\nabla})}{2\rho_0}\delta\rho = J_s\nabla^2\left[-J_s g\frac{\nabla^2\delta\rho}{2\rho_0} + \delta\rho\right]. \tag{2.16}$$

Rewriting and neglecting $O(\nabla^4)$ terms gives

$$\frac{\hbar^2}{2\rho_0}\left[\partial_t^2 + 2\partial_t(\boldsymbol{v_s} \cdot \boldsymbol{\nabla}) + (\boldsymbol{v_s} \cdot \boldsymbol{\nabla})^2\right]\delta\rho - J_s\nabla^2 g\delta\rho = 0. \tag{2.17}$$

From this equation we can deduce the velocity of the spin waves. If the drift velocity equals zero, the wave equation appears. So now we define the velocity of spin-waves c as $c^2 \equiv 2J_s g\rho_0/\hbar^2$ to construct the matrix

$$f^{\mu\nu} \equiv \frac{c^2}{J_s g}\begin{pmatrix} 1 & v_x & v_y & v_z \\ v_x & v_x^2 - 2c^2\rho_0/\hbar^2 & v_x v_y & v_x v_z \\ v_y & v_x v_y & v_y^2 - 2c^2\rho_0/\hbar^2 & v_y v_z \\ v_z & v_x v_z & v_y v_z & v_z^2 - 2c^2\rho_0/\hbar^2 \end{pmatrix}, \tag{2.18}$$

and we write Eq. 2.17 in the form

$$\partial_\mu(f^{\mu\nu}\partial_\nu\delta\rho) = 0. \tag{2.19}$$

From this equation the analogy with gravity can be seen as Warsen showed in his thesis [8]. He showed that such an equation can be expressed in the same form as the Schwarzschild metric for a gravitational black hole. Now that the analogy of spin-waves in an induced current with gravity is clear, we now construct two different shaped models and map their current densities so we can determine the location and shape of the horizon.

3 The horizon

To create an analogue black hole horizon we consider a two dimensional sheet made of iron. A two dimensional system is easier to work with and still useful for experimental purposes. This is because magnetic conductors are usually made out of many thin layers. Iron is a convenient material since it is both ferromagnetic and conductive. An electric field is applied to the system so that current flows through it. When narrowing the geometry of the iron sheet, the current density increases and therefore the drift velocity associated with it. When there is no drift velocity, the magnons velocity is equal to c. If the magnons are heading in the direction opposite of the flowing electrons with drift velocity v_s, two regions arise. The regions are given by $v_s > c$ and $v_s < c$. At the boundary $v_s = c$, the horizon is located. One can think of the spin-waves traveling on the stream electrons, where there exist a critical

point where the spin-waves cannot exceed the velocity of the stream. At this point, the spin waves are restricted to the region where $v_s > c$ and cannot escape it.

In Eq. 2.3 we see that the drift velocity only depends on the current density, since all the terms in front of $\boldsymbol{j}$ are constant for a given material. So searching for a critical velocity v_c, where $v_s = c$, is equivalent to searching the critical current density j_c corresponding to v_c. Duine *et al.* estimated the critical current density at a value of 10^{11} A/m^2 [7]. In the figure below, a visualization of the magnonic black hole is made. In the next section we derive a set of partial differential equation which applies to electrical circuits which the model must comply to.

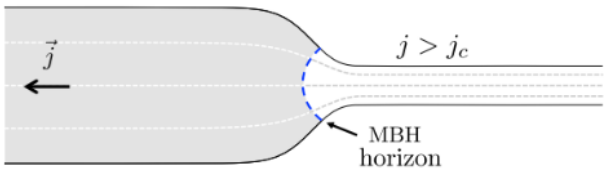

Figure 2: Schematically figure of a magnonic black hole for spin-waves incoming from the left. Taken from [7].

3.1 Laplace equation

To determine the drift velocity in our electrical circuit, we need to determine the current density in our system. Since our system is of uniform material, it will have a constant conductivity. This constant conductivity will allow us to make use of the approximated relation [11]

$$\boldsymbol{j} = \sigma \boldsymbol{E}, \tag{3.1}$$

where σ is the electrical conductivity and $\boldsymbol{E}$ the electric field. Rewriting $\boldsymbol{j}$ in terms of $\boldsymbol{E}$ allows us to express $\boldsymbol{j}$ in terms of electrical potential V. Since the electric field is conservative the relation $\boldsymbol{E} = -\boldsymbol{\nabla} V$ holds and we write

$$\boldsymbol{j} = -\sigma \boldsymbol{\nabla} V. \tag{3.2}$$

This shifts the problem of finding the vector field $\boldsymbol{j}$ to finding the scalar function of V.

Since charge cannot flow out of a conductor, the boundary condition [11]

$$\boldsymbol{n} \cdot \boldsymbol{j} = 0, \tag{3.3}$$

where $\boldsymbol{n}$ is the normal vector, must hold. Furthermore, the continuity equation must hold, since charge must be conserved in the conductor. This means that [11]

$$\boldsymbol{\nabla} \cdot \boldsymbol{j} = 0. \tag{3.4}$$

Making use of Eq. 3.2 allows us to rewrite Eq. 3.3 as

$$\boldsymbol{n} \cdot \boldsymbol{\nabla} V = 0, \tag{3.5}$$

and Eq. 3.4 as

$$\Delta V = 0. \tag{3.6}$$

With Eq. 3.5 and Eq. 3.6 we now have a set of partial differential equations. We can apply these equations to different models to obtain an unique current density. In the next section we will specify the chosen models and show the corresponding current densities. We also specify where the current density equals the critical current density to determine the shape of the horizon.

3.2 Magnonic black hole model 1

Our first model has the same shape as figure 2 and can be specified by four boundaries. In this thesis, we only focus on the part where the model is narrowed and the horizon is located. The boundaries $x = 0$ and $x = L$ represents the regions where current can flow through. At these boundaries, the model can be expanded to eventually create a closed electrical circuit. We set the potential energy of the boundary at $x = 0$ equal to zero and set the boundary at $x = L$ at a potential $V = 4 * 10^{-5}$J/C. The other two boundaries are given by $y = Cos[\pi x/L] + 2$ and $y = -Cos[\pi x/L] - 2$ and represent the edges of the model. Therefore, they must obey the boundary condition in Eq. 3.3. For this model we choose a value of $L = 3$, $L = 4$ and $L = 5$. The models for $L = 3$ and $L = 5$ are shown in the appendix. All length units are in nm which is a common length scale in nanofabrication techniques.

In figure 3a, the distribution of the current density for the model of length scale $L = 4$ is visualized. We see that narrowing the width of the electrical circuit leads to an increase in current density. Also note that the outer most vectors are aligned with the boundary. This implies that no current is flowing out and that the boundary condition in Eq. 3.3 is satisfied. In figure 3b, the results for the same model are plotted differently, where the values of the current density are given by means of color scale. In this figure, three lines are given. The brown line represents the critical current density j_c, the black line $0.9 * j_c$ and the purple line $1.1 * j_c$. The brown line which represents j_c is the magnonic black hole horizon. However, the value of j_c is not known to a high accuracy, so a slightly higher and lower value of j_c are displayed to take this uncertainty into account. We see that the horizon is curved smoothly, where the degree of curvature depends on the exact value of j_c. The same three lines are shown in figure 4 and represent the same values. In this plot we see an intersection of the model at $y = 0$. The blue line represents the current density in the model. The current density equals $0.9 * j_c$ at $x = 1.90425$ nm, j_c at $x = 2.26575$ nm and $1.1 * j_c$ at $x = 2.57104$ nm. These values represent the location of the magnonic black hole horizon at $y = 0$, depending on the value of j_c. In figures 7 and 8 in the appendix, the model is displayed for length scales $L = 3$ and $L = 5$, respectively. From this, we see that when the length scale is reduced, the system narrows faster. This leads to a increase in current density. We conclude that magnons incoming from the left will enter the horizon more quickly.

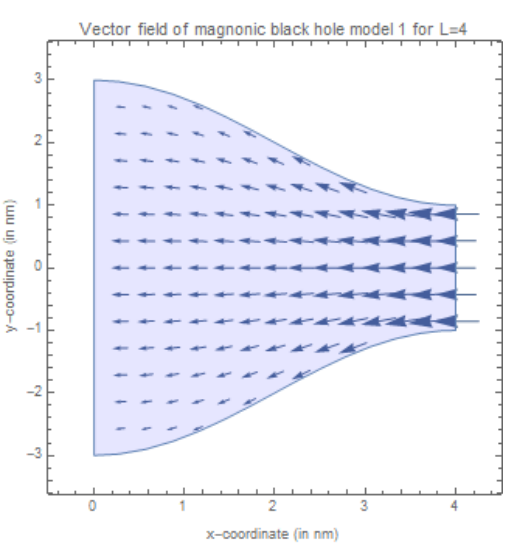

(a) Vectorfield

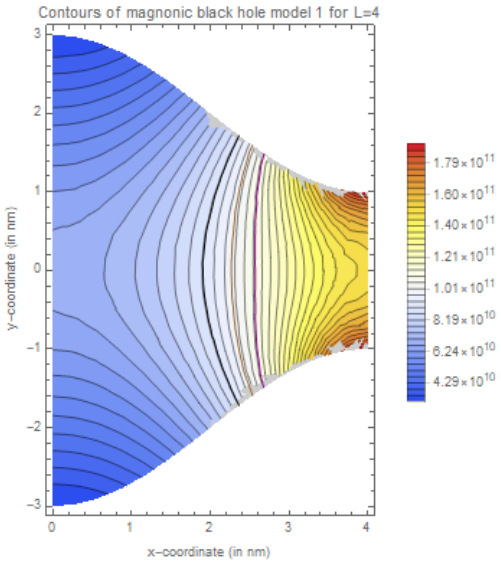

(b) Contourplot

Figure 3: Figure a shows the direction in which the current is flowing for a magnonic black hole model. Here, the potential is set at a value of $V = 0$ at the left boundary and $V = 4{*}10^{-5}$ J/C at the right boundary. Bigger arrows represents higher current densities. Figure b shows the values of the current density of the same model. In this figure, the lines represents contours, where the black line equals a value of $0.9 * j_c$, the brown line j_c and the purple line $1.1 * j_c$, where the critical current density $j_c = 10^{11}\text{A/m}^2$ and represents the magnonic black hole horizon. The red area represents a high current density, whereas the blue are represents a low current density as indicated in the legend, which is expressed in A/m^2.

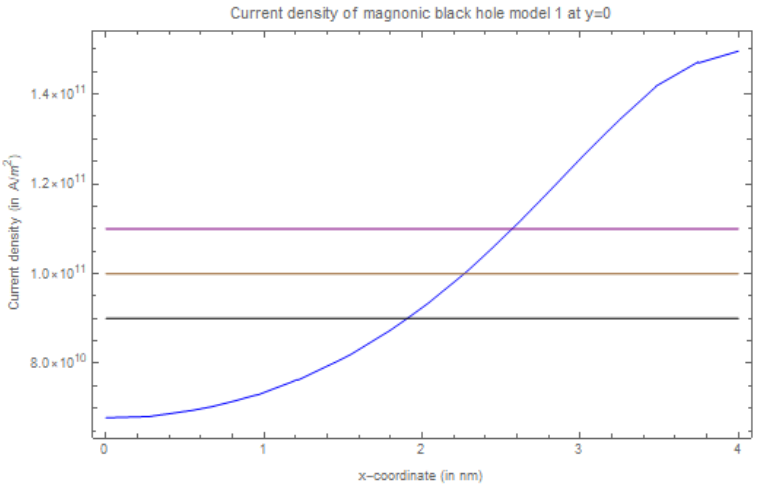

Figure 4: This figure shows the current density of magnonic black hole model 1 at $y = 0$. The current density is given in blue, the black line equals a value of $0.9 * j_c$, the brown line j_c and the purple line $1.1 * j_c$, where j_c is the critical current density and equals a value of 10^{11}A/m^2. The critical current density is where the magnonic black hole horizon is located.

3.3 Magnonic black hole model 2

Our second model can be described by 4 boundaries. The first two boundaries are give by $x = 0$ and $x = L$ and have a potential of $V = 0$ J/C and $V = 4 * 10^{-5}$ J/C respectively. The last two boundaries are given by $y = x/L - 2$ and $y = -x/L + 2$. Again, the first two boundaries represent the regions where current can flow through, in contrast to the last two boundaries, where the boundary condition in Eq.3.3 must hold. For this model we make use of length scales $L = 3.5$, $L = 4$ and $L = 4.5$. The models of length scales $L = 3.5$ and $L = 4.5$ are shown in the appendix. The length scales are again given in nm. For this model of length scale $L = 4$, figure 5a shows the direction of the current flowing and in figure 5b the values of the current density are given. Again the three lines represent the values $0.9 * j_c$, j_c and $1.1 * j_c$. In figure 6 the current density of model 2 is given for $y = 0$. The lines intersect the current density at $x = 1.51473$ nm, $x = 2.20931$ nm and $x = 2.76673$ nm. Again, this is where the magnonic black hole horizon is located at $y = 0$, depending on the value of j_c. We see that the horizon is once again smoothly curved. In figures 9 and 10 in the appendix, the model is shown for length scales $L = 3.5$ and $L = 4.5$, respectively. From these figures we see that this model is more sensitive to the value of L than model 1. Also, this model is more sensitive for the value of j_c, since the three horizons are further apart from each other.

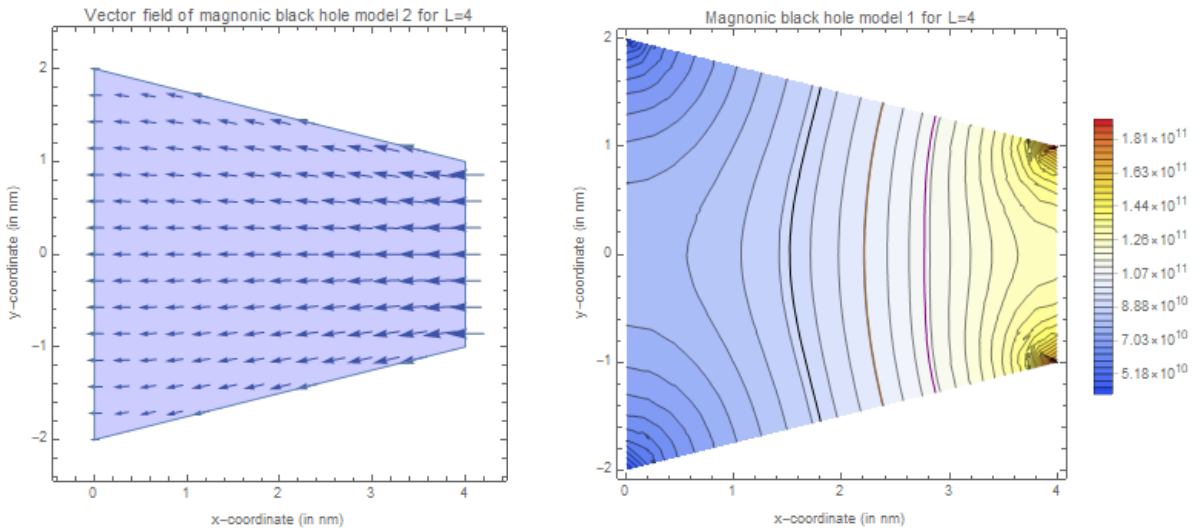

(a) Vectorfield (b) Contourplot

Figure 5: Figure a shows the direction current is flowing for a magnonic black hole model, where the potential is set at a value of $V = 0$ at the left boundary and $V = 4 * 10^{-5}$ J/C at the right boundary. Bigger arrows represents higher current densities. Figure b shows the values of the current density of the same model. In this figure, the lines represents contours, where the black line equals a value of $0.9 * j_c$, the brown line j_c and the purple line $1.1 * j_c$, where $j_c = 10^{11}$ A/m^2. The brown line represents the magnonic black hole horizon. The red area represents a high current density, whereas the blue are represents a low current density as indicated in the legend, which is expressed in A/m^2.

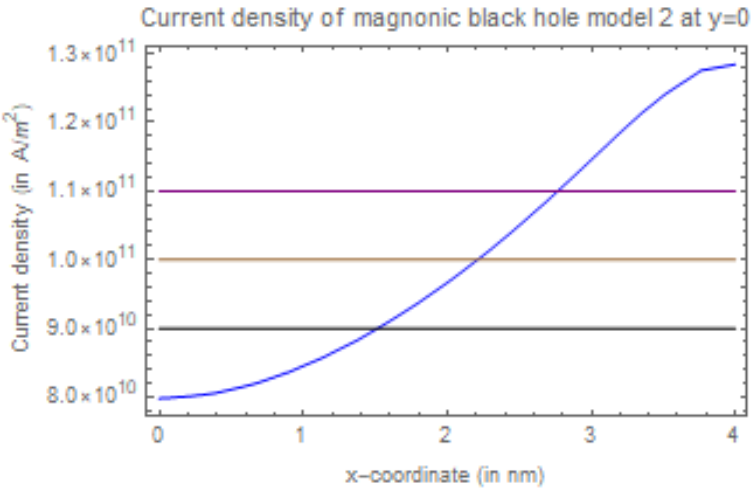

Figure 6: This figure shows the current density of magnonic black hole model 2 at $y = 0$. The current density is given in blue, the black line equals a value of $0.9 * j_c$, the brown line j_c and the purple line $1.1 * j_c$, where $j_c = 10^{11}$ A/m^2. The intersection of the brown and blue line is where the magnonic black hole horizon is located.

4 Discussion and Outlook

In this thesis we derived from the LLG equation the velocity of spin waves in a ferromagnetic material under the influence of an electrical current. In the electrical circuit, spin-waves cannot exceed the drift velocity if the circuit is narrowed enough, which results in a region where the spin-waves cannot escape it anymore. The interface where the drift velocity equals the velocity of the spin waves is where the 'point of no return' is located, which is called the horizon. We set up two different models to monitor the current density so we can determine the shape of the horizon. In both models, the horizon is smoothly curved, where the degree of curvature and the location of the horizon depends on the value of the critical current density.

We now discuss some approximations. First of all, in Eq.2.1, the dissipative terms were neglected. In first order, neglecting the dissipative terms still leads to useful insights in the shape of a magnonic black hole horizon. However, including the terms will lead to greater exactness. Furthermore, although the boundary condition of current not being allowed to flow out of the system is stated in Eq.3.3, the boundary condition is not implemented in the simulation. The code would not work with the boundary condition applied explicitly. However, as can bee seen in figures 3a and 5a the current on the edges does align with the boundary. Calculating the outflow of current at the boundary lead to significantly low values. It is at the corners where the outflow became increasingly significant. This problem can be solved by implementing the boundary condition in the model. Also, it might help to extend the curved boundaries into horizontal edges.

In this thesis, we computed the shape and location of the magnonic black hole horizon. For both models, we gave three possible horizons, since the value of the critical current density is not known with high accuracy. To determine the actual shape and position of a magnonic black hole horizon, the value of the critical current density must be known to a higher level of precision. To know the exact location and shape is important to measure properties like Hawking and Cherenkov radiation, since they are produced at the horizon. Therefore, the details on the shape and location must increase significantly before experimental testing can lead to useful results.

References

[1] S. Schaffer, Journal for the History of Astronomy **10**, 42 (1979).

[2] B. P. Abbott, R. Abbott, T. Abbott, M. Abernathy, F. Acernese, K. Ackley, C. Adams, T. Adams, P. Addesso, R. Adhikari, et al., Physical review letters **116**, 061102 (2016).

[3] K. Akiyama, A. Alberdi, W. Alef, K. Asada, R. Azulay, A.-K. Baczko, D. Ball, M. Baloković, J. Barrett, D. Bintley, et al., The Astrophysical Journal Letters **875**, L4 (2019).

[4] W. G. Unruh, Physical Review Letters **46**, 1351 (1981).

[5] O. Lahav, A. Itah, A. Blumkin, C. Gordon, S. Rinott, A. Zayats, and J. Steinhauer, Physical review letters **105**, 240401 (2010).

[6] G. Rousseaux, C. Mathis, P. Maïssa, T. G. Philbin, and U. Leonhardt, New Journal of Physics **10**, 053015 (2008).

[7] A. Roldán-Molina, A. S. Nunez, and R. Duine, Physical review letters **118**, 061301 (2017).

[8] N. Warsen, B.Sc. thesis (2018).

[9] S. Claerhoudt, B.Sc. thesis (2018).

[10] S.-K. Kim, Journal of Physics D: Applied Physics **43**, 264004 (2010), URL `https://doi.org/10.1088%2F0022-3727%2F43%2F26%2F264004`.

[11] D. J. Griffiths, *Introduction to electrodynamics* (2005).

A Appendix

A.1 Figures

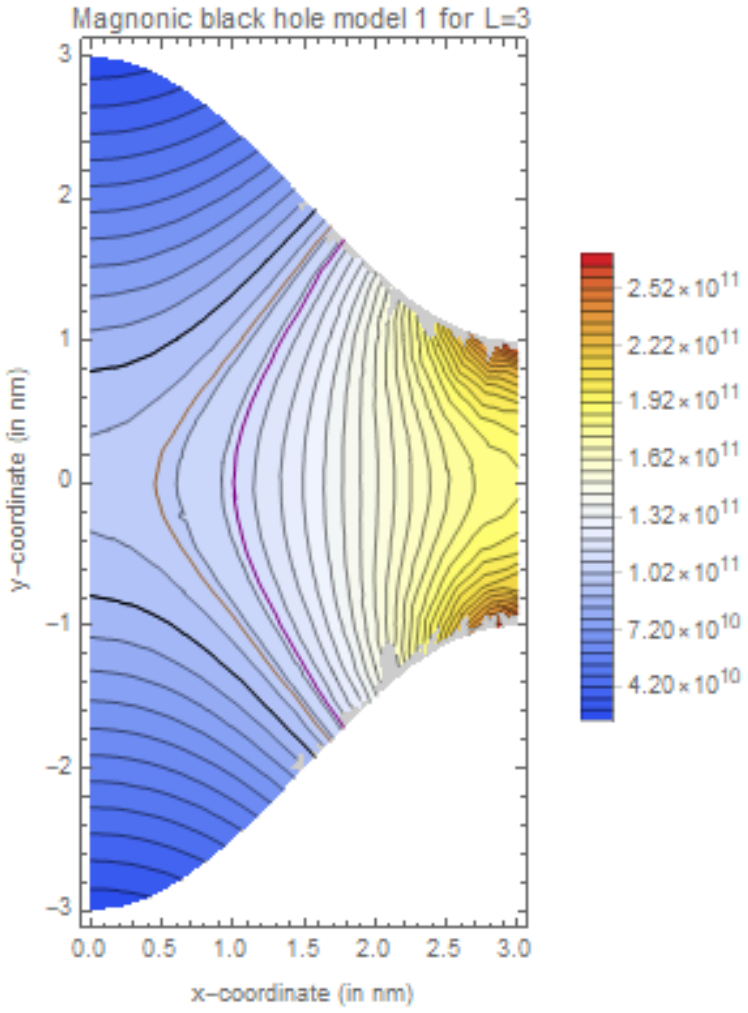

Figure 7: This figure shows the current density of a magnonic black hole model. In this figure, the lines represents contours, where the black line equals a value of $0.9 * j_c$, the brown line j_c and the purple line $1.1 * j_c$, where the current density $j_c = 10^{11}$ A/m^2. The brown line represents the magnonic black hole horizon. The red area represents a high current density, whereas the blue are represents a low current density as indicated in the legend, which is expressed in A/m^2.

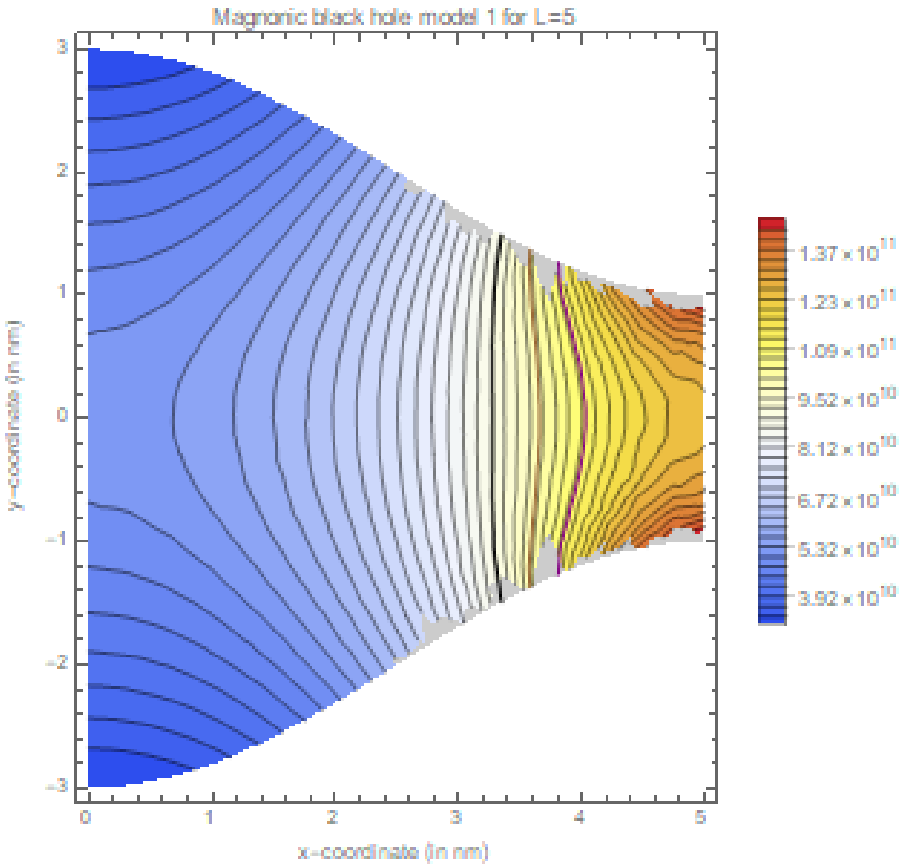

Figure 8: This figure shows the current density of a magnonic black hole model. In this figure, the lines represents contours, where the black line equals a value of $0.9 * j_c$, the brown line j_c and the purple line $1.1 * j_c$, where the current density $j_c = 10^{11}$ A/m^2. The brown line represents the magnonic black hole horizon. The red area represents a high current density, whereas the blue are represents a low current density as indicated in the legend, which is expressed in A/m^2.

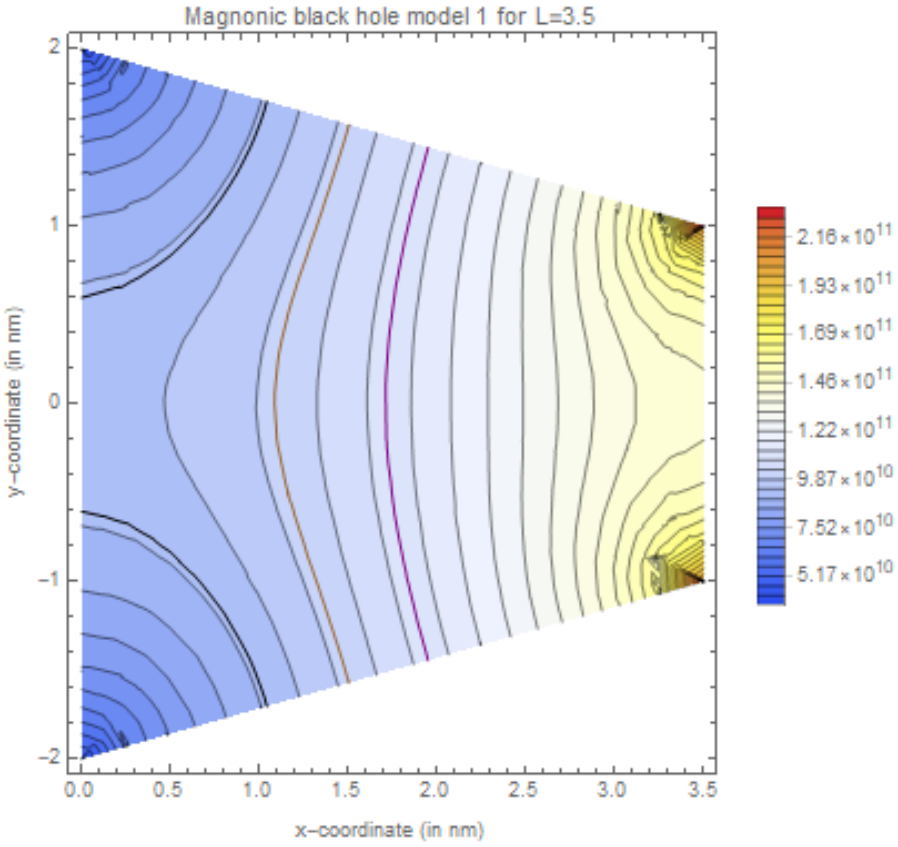

Figure 9: This figure shows the current density of a magnonic black hole model. In this figure, the lines represents contours, where the black line equals a value of $0.9 * j_c$, the brown line j_c and the purple line $1.1 * j_c$, where the current density $j_c = 10^{11}$ A/m^2. The brown line represents the magnonic black hole horizon. The red area represents a high current density, whereas the blue are represents a low current density as indicated in the legend, which is expressed in A/m^2.

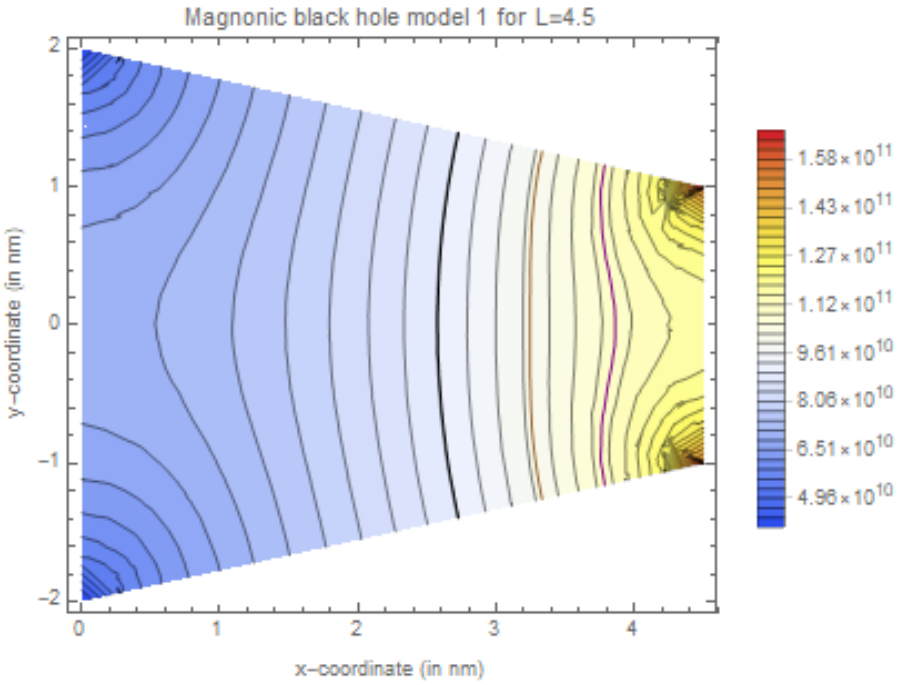

Figure 10: This figure shows the current density of a magnonic black hole model. In this figure, the lines represents contours, where the black line equals a value of $0.9 * j_c$, the brown line j_c and the purple line $1.1 * j_c$, where the current density $j_c = 10^{11}$ A/m^2. The brown line represents the magnonic black hole horizon. The red area represents a high current density, whereas the blue are represents a low current density as indicated in the legend, which is expressed in A/m^2.